Research Article

Copper Corrosion Inhibition in 1 M Nitric Acid: Adsorption and Inhibitive Action of Theophylline

V. Kouakou, P. M. Niamien*, A. J. Yapo, and A. Trokourey

Laboratoire de Chimie Physique, Université Félix Houphouët Boigny, Abidjan (Cocody)

Abstract

The corrosion inhibition of copper in 1.0M HNO_3 solution by theophylline (TP) has been studied in the temperature range of 308-328K and the concentration range of 0.1-5mM, using mass loss measurement technique. The results indicate that (TP) inhibited the corrosion reaction in the acid medium and inhibition efficiency is concentration and temperature dependent. The adsorption of (TP) on copper follows the modified Langmuir isotherm. The adsorption thermodynamic functions (ΔG^0_{ads}, ΔH^0_{ads}, and ΔS^0_{ads}) and the activation parameters (E_a, ΔH_a*, ΔS_a*) were determined and their values suggest both physisorption and chemisorption processes. Theoretical studies have been performed using quantum chemical calculations. Density functional theory (DFT) at different levels has been used with 6-31G (d) basis set in order to elucidate adsorption and reactive sites of the compound. The calculated quantum chemical parameters correlated to the inhibition efficiency are the frontier molecular orbital energies E_{HOMO} (highest occupied molecular orbital energy), E_{LUMO} (lowest unoccupied molecular orbital energy), energy gap (ΔE), dipole moment (μ) and other parameters including global hardness (η), global softness (S), absolute electronegativity (χ), electrophilicity index (ω) and the fraction of electrons transferred (ΔN) from the inhibitor molecule to the metal. The local reactivity has been analyzed through the condensed Fukui function and condensed softness indices using Mulliken population analysis. The calculated results are in agreement with the experimental data.

Keywords: Copper; nitric acid; theophylline; corrosion inhibition; mass loss technique; quantum chemical parameters; Fukui indices

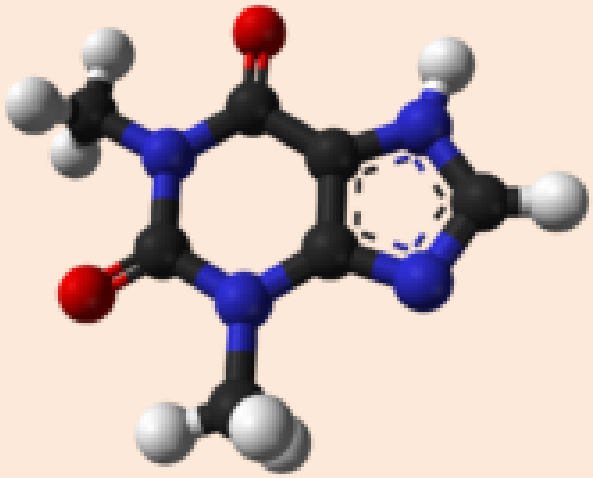

***Correspondence**

Author: P. M. Niamien

Email: niamienfr@yahoo.fr

Introduction

The corrosion phenomenon of materials [1] is an important topic in many industries because of its consequences on industrial equipment including vessels, engineering vehicles, mining equipment, packaging machineries, etc. Corrosion mostly involves the deterioration of the materials and it is widely common in metals. The use of inhibitors [2] is one of the most practical methods to protect metals against corrosion, especially in acidic media. Most of the organic inhibitors [3, 4] containing nitrogen, oxygen, sulphur atoms, and multiple bonds in their molecules facilitate adsorption on the metal surface. Many researchers [5] conclude that the adsorption on the metal surface depends mainly on the physicochemical properties of the inhibitor, such as the functional group, molecular electronic

structure, electron density at the donor atom, π orbital character and the molecular size. The planarity and the lone electron pairs in the heteroatoms [6] are important features that determine the adsorption of molecules on the metallic surface.

A large number of organic compounds [7-9] have been investigated as corrosion inhibitors for different types of metals. With increased awareness towards environmental pollution and control, the search for less toxic and environmentally friendly corrosion inhibitors are becoming increasingly important. Thus, researchers focused their works on several drugs, including molecules in the class of β-lactam antibiotics [10, 11], cephalosporins [12], quinolones [13-15], antifungal drugs [16], etc.

Quantum chemical calculations have been widely used to study reactive mechanism and to elucidate many experimental observations. They have been proved [17, 18] to be a very powerful tool for studying corrosion inhibition mechanism. Density functional theory (DFT) [19, 20] has provided a very useful framework for developing new criteria for rationalizing, predicting and eventually understanding many aspects of chemical processes [21, 22]. During the last decades, density functional theory has undergone fast development, especially in the field of organic chemistry, as the number of accurate exchange-correlation functionals increased. Indeed, the apparition of gradient corrected and hybrid functionals in the late 1980s greatly improved the chemical accuracy of the Hohenberg–Kohn theorem [19] based methods. The Kohn–Sham formalism [23] and its density-derived orbitals paved the way to computational methods. In parallel, a new field of application of DFT developed, the so-called conceptual DFT [24]. Parr and Yang followed the idea that well-known chemical properties as electronegativity, chemical potentials and affinities could be sharply described and calculated manipulating the electronic density as the fundamental quantity [25, 26]. Moreover, starting from the work of Fukui and its frontier molecular orbitals (FMOs) theory [27], the same authors further generalized the concept and proposed the Fukui function as a tool for describing the local reactivity in molecules [28].

The aim of this paper is to explore the use of theophylline as an acid corrosion inhibitor for copper in nitric acid solution, using mass loss technique and to analyze the inhibition efficiency in the light of the global and local quantum chemical parameters.

Experimental

Materials and Reagents

Copper specimens

The copper specimens were in the form of rod measuring 10 mm in length and 2.2 mm in diameter; they were cut in commercial copper of purity 95%.

The studied molecule

Theophylline (formula $C_7H_8N_4O_2$) structure is given in **Figure 1**.

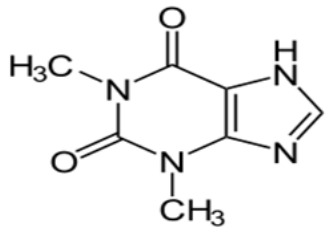

Figure 1 Chemical structure of Theophylline

Solution

Analytical grade, 65% nitric acid solution from Merck was used to prepare the corrosive aqueous solution. The solution was prepared by dilution of the commercial nitric acid solution using double distilled water. The blank was a 1 M HNO_3 solution. Theophylline of analytical grade was acquired from Sigma Aldrich chemicals and solutions range from 0.1 to 5mM were prepared.

Mass loss measurements

The mass loss method [29, 30] is the most widely used methods of inhibition assessment. The simplicity and reliability of the measurement offered by mass loss method [31, 32] is such that the technique forms the baseline method of measurement in many corrosion monitoring programs. Mass loss experiments were conducted at the range of temperature 308-328K by completely immersion of the polished copper specimens in nitric acid 1.0 M solution without and with different concentrations of theophylline. A total immersion time of 1h was recorded. From the mass loss measurements, parameters such as the inhibition corrosion rate (W), surface coverage (θ) and inhibition efficiency IE (%) were calculated using the equations below:

$$W = \frac{\Delta m}{St} \quad (1)$$

$$\theta = \frac{W_0 - W}{W_0} \quad (2)$$

$$IE(\%) = \frac{W_0 - W}{W_0} \times 100 \quad (3)$$

Where W_0 and W are respectively the corrosion rate without and with theophylline, Δm is the mass loss, S is the total surface of the copper specimen and *t* is the immersion time.

Computational details

In order to explore the theoretical - experimental consistency, quantum chemical calculations were performed using Gaussian 03 W software package [33]. Calculations on the investigated molecule were performed using Density Functional Theory (DFT) with different hybrid functionals including B3LYP (Becke's three parameter hybrid functional [34] with the correlation functional of Lee, Yang and Parr [35, 36]), B3PW91 (Becke's three parameter hybrid functional with the correlation functional of Perdew and Wang [37]) and PBEPBE (Perdew, Burke and Ernzerhof [38]) with 6-31G (d) basis set.

Results and discussion

Mass loss studies were performed in the absence and presence of theophylline. The concentration in that molecule ranges from 0.1 to 5mM. The temperature varies from 308 to 328K. The increase in theophylline concentration is accompanied by a decrease in corrosion rate (**Figure 2**) and increase in inhibition efficiency (**Figure 3**). These results show that theophylline acts as an inhibitor of copper corrosion in 1M HNO_3.

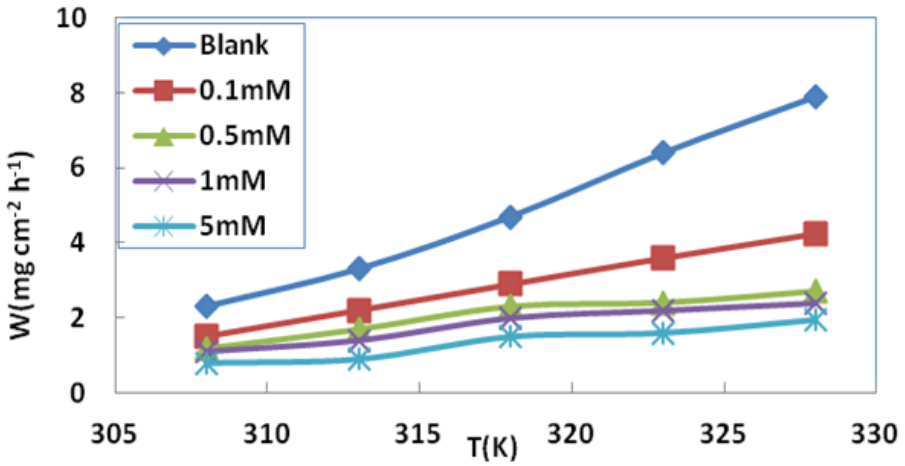

Figure 2 Evolution of corrosion rate with temperature for different concentrations

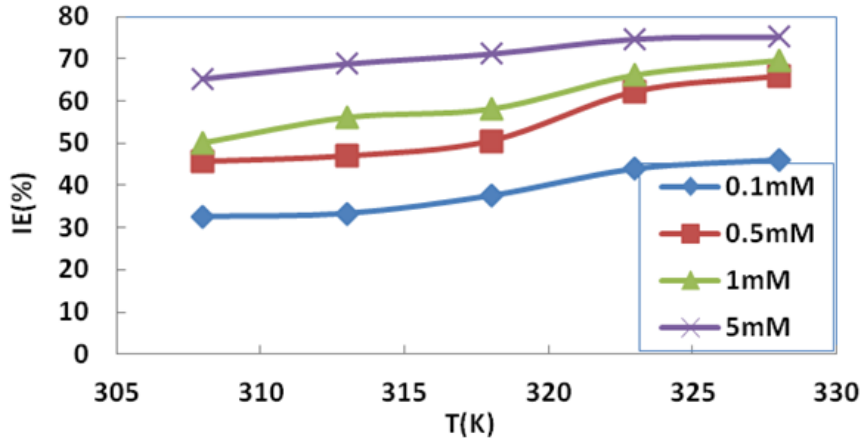

Figure 3 Inhibition efficiency versus temperature for different concentrations

The observed behavior of Theophylline could be explained by an increase in its adsorption on copper surface when temperature increases. It is widely acknowledged [39] that the adsorption isotherms provide useful insights into the mechanism of corrosion inhibition. It is then necessary to determine empirically which adsorption isotherm fits best to the surface coverage data in order to use the corrosion rate measurements to evaluate thermodynamic parameters pertaining to the inhibitor's adsorption. Adsorption isotherms are generally of the form [40]:

$$f(\theta, x)\exp(-2a\theta) = K_{ads}C_{inh} \qquad (4)$$

$f(\theta, x)$ is the configurational factor that depends essentially on the physical model assumptions underlying the derivation of the isotherm and *a* is the molecular interactions parameter depending upon molecular interactions in the adsorption layer and the degree of heterogeneity of the surface. Attempts were made to fit the values of the degree of surface coverage(θ), which represents the part of metal surface covered by the adsorbate to three isotherms including Langmuir, Flory Huggins and El-Awady. Table 1 gives the equations of the isotherms.

In the expressions in **Table 1**, *x* is the number of water molecules replaced by one molecule of organic adsorbate; C_{inh} is the inhibitor concentration in the bulk of the solution. K_{ads} is the equilibrium constant of the adsorption process. The magnitude of K_{ads} is directly proportional to the inhibition efficiency. In general, K_{ads}, the equilibrium adsorption constant, represents the adsorption power or binding strength of the inhibitor molecule on the metal surface.

Values of *1/y* less than one [41] imply the formation of a multilayer of the inhibitor on the metal surface and *1/y* greater than one means that the inhibitor molecule will occupy more than one active site. The plots of these isotherms are given in **Figures 4, 5** and **6**. The choice of the best inhibitor was based on the values of the correlation coefficients of the plots. **Table 2** gives the parameters of the studied models.

Table 1 Equations of the tested adsorption isotherms

Isotherm	Equation
Langmuir	$\frac{C_{inh}}{\theta} = \frac{1}{K_{ads}} + C_{inh}$
Flory Huggins	$log\,(\theta/C_{inh}) = logxK + xlog(1-\theta)$
El-Awady	$log[\theta/(1-\theta)] = logK' + ylogC_{inh}(K_{ads} = K'^{1/y})$

One can see from table 2 that Langmuir adsorption isotherm is by far the best adsorption isotherm. Ideally, these plots should yield unit slopes, the linearity of the plots may be taken to mean that theophylline adsorption on copper obeys the Langmuir model, but the considerable deviation of the slopes from unity shows that the isotherm cannot be strictly applied in the description of the adsorption parameters. This deviation from unity [41] is attributed to the

interactions between adsorbate species on the metal surface as well as changes in the adsorption heat with increasing surface coverage. Therefore, a modified Langmuir equation suggested elsewhere [42] may be used:

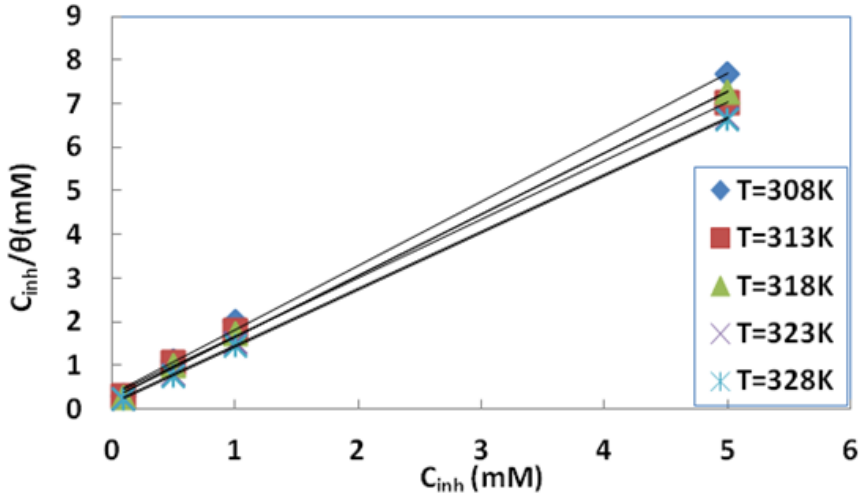

Figure 4 Langmuir adsorption isotherm for different concentrations

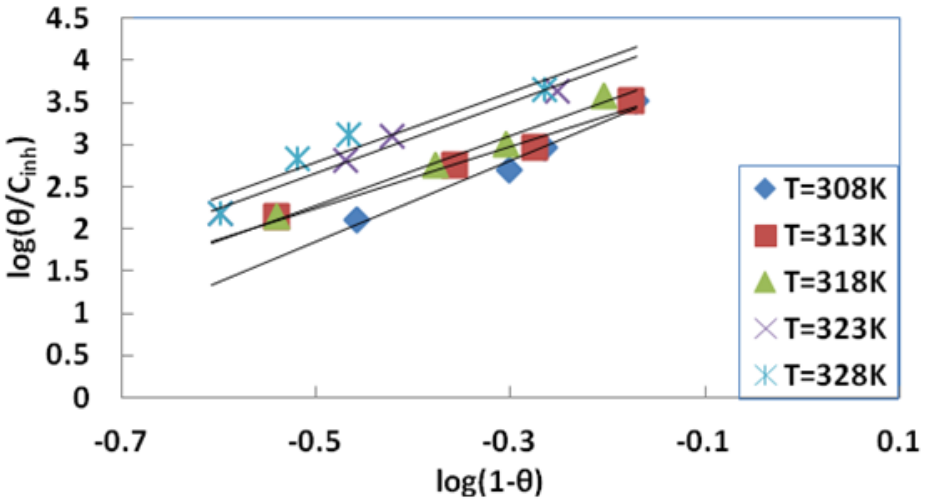

Figure 5 Flory Huggins adsorption isotherms for different concentrations

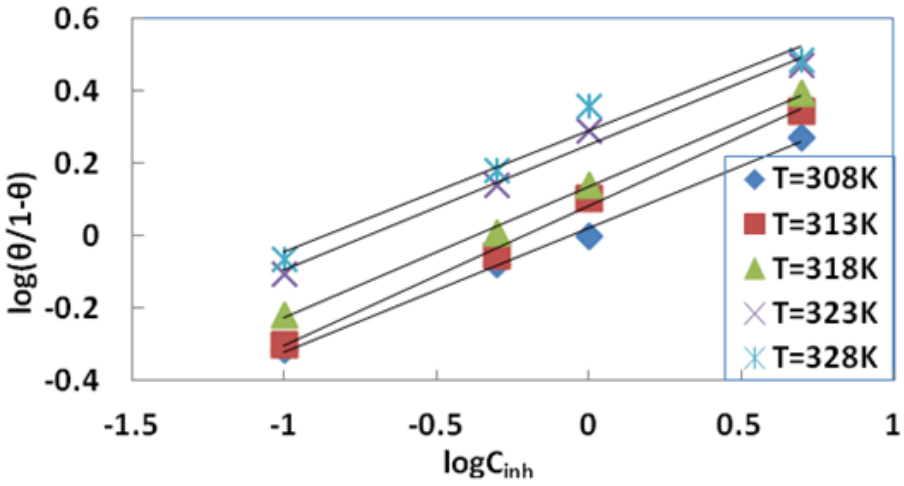

Figure 6 El-Awady adsorption isotherms for different concentrations

Table 2 Adsorption isotherms parameters

Isotherm	T(K)	R^2	Slope	Intercept
Langmuir	308	0.998	1.473	0.3359
	313	0.998	1.345	0.3231
	318	0.999	1.410	0.2343
	323	0.999	1.310	0.1455
	328	1.000	1.307	0.1053
Flory Huggins	308	0.997	4.787	4.2529
	313	0.980	3.657	4.0783
	318	0.986	4.132	4.3491
	323	0.981	4.219	4.7715
	328	0.907	4.139	4.8643
El-Awady	308	0.996	0.343	0.0222
	313	0.995	0.384	0.0818
	318	0.998	0.363	0.1357
	323	0.988	0.343	0.2517
	328	0.956	0.332	0.2895

$$\frac{C_{inh}}{\theta} = \frac{n}{K_{ads}} + nC_{inh} \qquad (5)$$

The values of K_{ads} were then calculated using the intercepts of the straight lines on C_{inh}/θ-axis. The equilibrium constant was related to the standard free adsorption enthalpy by the following equation [43]:

$$\Delta G^0_{ads} = -RTln(55.5K_{ads}) \qquad (6)$$

In the above equation [42], 55.5 is the concentration of water in mol L^{-1}. The values of ΔG^0_{ads} are summarized in **Table 3**.

Table 3 Adsorption thermodynamic functions

T(K)	K_{ads} ($\times 10^3$ M^{-1})	ΔG^0_{ads} (kJmol^{-1})	ΔH^0_{ads} (kJmol^{-1})	ΔS^0_{ads} (Jmol^{-1}K^{-1})
308	2.977	-30.75		
313	3.095	-31.35		
318	4.268	-32.70	52.6	269.2
323	6.873	-34.49		
328	9.500	-35.91		

Adsorption of organic compounds onto metal surfaces may occur by electrostatic interactions between charged species and the charged metal or by interactions of π electrons of the molecule with the metal, or both. In any case the strength of interactions between the adsorbate and the adsorbent is often revealed in the values of the adsorption-desorption equilibrium constant. The computed values of free adsorption enthalpy change, ΔG^0_{ads} were negative, indicating a spontaneous nature of the adsorption of theophylline on copper.

Literature [43, 44] suggests that values of ΔG^0_{ads} around-40 kJ mol^{-1} or more negative are associated with chemisorption while those of -20 kJ mol^{-1} or less negative indicate physisorption. The computed values in table 3 seem to indicate both chemisorption and physorption. The standard adsorption enthalpy change ΔH^0_{ads} and the standard adsorption entropy change ΔS^0_{ads} are correlated with standard Gibbs free energy by the relation:

$$\Delta G^0_{ads} = \Delta H^0_{ads} - T\Delta S^0_{ads} \qquad (7)$$

Figure 7 gives the plots of ΔG^0_{ads} versus the temperature. The values of ΔH^0_{ads} and ΔS^0_{ads} obtained by linear regression are listed in table 3. ΔH^0_{ads} is positive, showing an endothermic process. The literature [45] pointed out that an exothermic process means either physisorption or chemisorption; while an endothermic process is associated to

chemisorption. ΔS^0_{ads} is positive, meaning that disorder increases during the adsorption process. This situation can be explained by the desorption of water molecules replaced by the inhibitor.

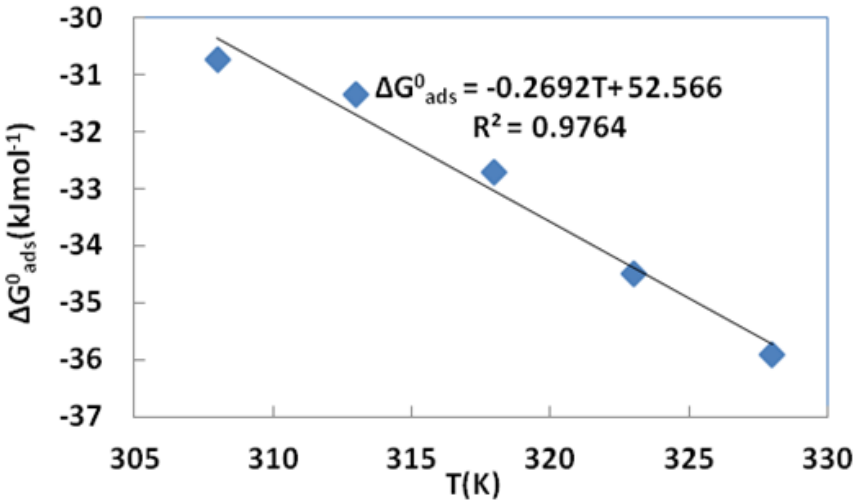

Figure 7 Free adsorption enthalpy ΔG^o_{ads} versus temperature

In order to distinguish between the two adsorption modes, experimental data were fitted to Dubinin Raduskhevich isotherm. This isotherm [46, 47] was first used to distinguish between physical and chemical adsorptions for removal of pollutants from aqueous solutions by adsorption on different adsorbents. It was [48] recently used to explain the mechanism of corrosion inhibition onto the metal surface in acidic solution. The basic equation of the model is:

$$ln\theta = ln\theta_{max} - a\delta^2 \qquad (8)$$

Where θ_{max} is the maximum surface coverage, and δ is the Polanyi potential which is given by:

$$\delta = RTln\left(1 + \frac{1}{C_{inh}}\right) \qquad (9)$$

In this relation, C_{inh} is expressed in g L^{-1}; R is the universal gas constant, T is the thermodynamic temperature. **Figure 8** gives the representation of $ln\theta$ versus δ^2. **Table 4** summarizes the plots parameters.

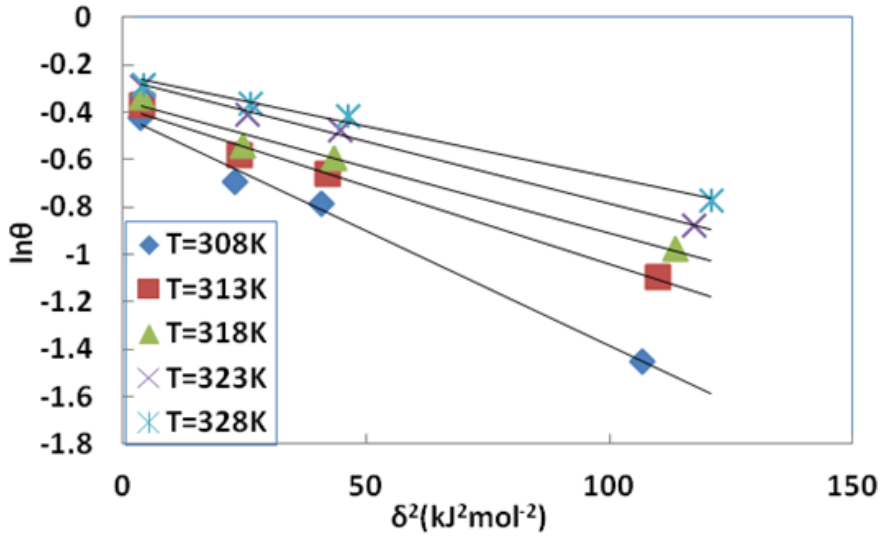

Figure 8 Dubinin Raduskhevich adsorption model plots for Theophylline on copper

Table 4 Regression parameters and adsorption mean energy of theophylline

T(K)	R^2	a ($kJ^2\ mol^2$)	$E^m_{ads}\ (kJ\ mol^{-1})$
308	0.941	0.0097	7.18
313	0.990	0.0066	8.70
318	0.980	0.0055	9.53
323	0.996	0.0052	9.80
328	0.992	0.0042	10.91

The mean adsorption energies were calculated using the following equation:

$$E^m_{ads} = \frac{1}{\sqrt{2a}} \qquad (10)$$

The magnitude of E^m_{ads} indicates the type of adsorption. Values of mean adsorption energy [48] less than 8 kJ mol^{-1} indicate physical adsorption. In this work the values of mean adsorption energies relative to the studied temperatures are included in the range of 7.18 to 10.91 what shows that we have both physisorption and chemisorption.

Kinetic and thermodynamic considerations

Arrhenius equation provides a mathematical dependency between the corrosion rates and temperature as follows:

$$logW = logA - \frac{E_a}{2.303RT} \qquad (11)$$

Where W is the corrosion rate, *A* is the Arrhenius pre-exponential constant, R is the molar gas constant and T is the absolute temperature. A plot of $logW$ versus $1/T$ yields a straight line (**Figure 9**) with slope as $(-E_a/2.303R)$ and intercept as $logA$.

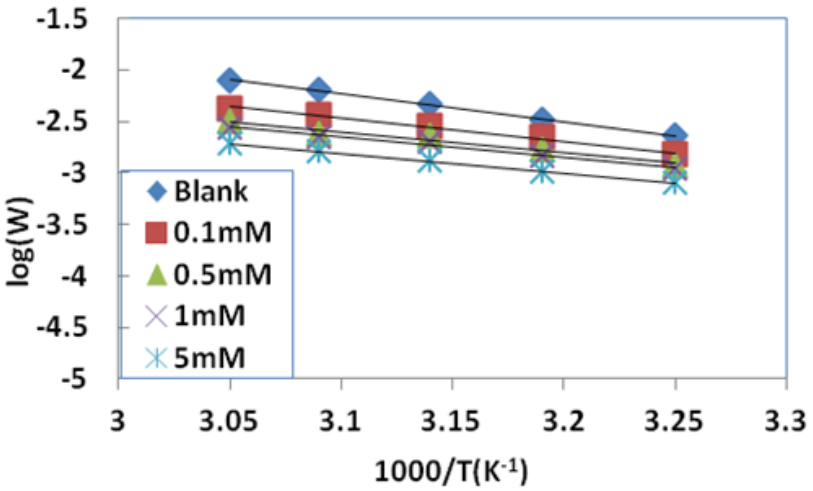

Figure 9 Arrhenius plots for copper corrosion in 1M HNO_3

In order to compute thermodynamic parameters such as change in activation enthalpy ΔH^*_a and change in activa, entropy ΔS^*_a, we use the transition state equation:

$$log\left(\frac{W}{T}\right) = \left[log\left(\frac{R}{Nh} + \frac{\Delta S^*_a}{2.303R}\right)\right] - \frac{\Delta H^*_a}{2.303RT} \qquad (12)$$

Where ΔS_a^* is the change in apparent activation entropy, ΔH_a^* is the change in apparent activation enthalpy, R is the perfect gas constant, $\aleph$ is the Avogadro number and h is the Planck's constant. **Figure 10** gives the plot of $log\left(\frac{W}{T}\right)$ versus $1/T$.

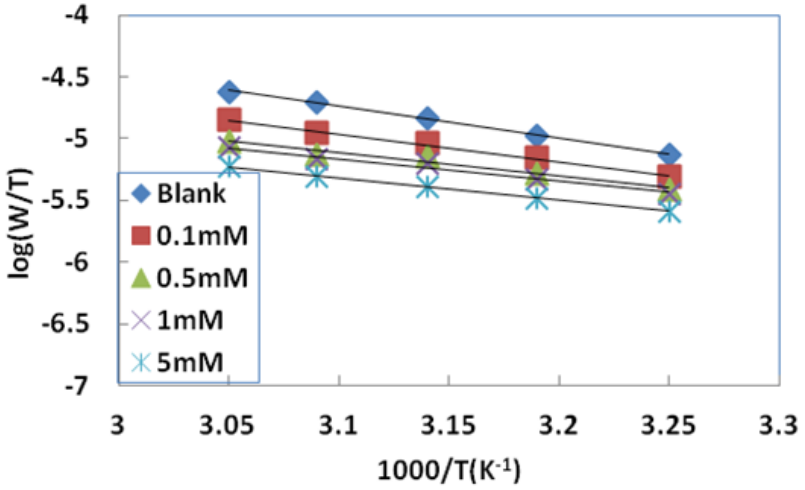

Figure 10 Transition state plots of the adsorption behavior of theophylline

The slope $(-\Delta H_a^*/2.303\,R)$ and the intercept $\log[(R/\aleph h) + (\Delta S_a^*/2.303R)]$ of each straight line lead to the values of activation enthalpy change and activation entropy change. All these values are displayed in **Table 5**.

Table 5 Kinetic/Thermodynamic parameters

System	$E_a\ (kJmol^{-1})$	$\Delta H_a^*\ (kJmol^{-1})$	$\Delta S_a^*\ (kJmol^{-1})$
Blank	52.1	49.4	-134.8
0.1mM	43.0	41.1	-159.1
0.5mM	37.6	35.6	-185.0
1mM	37.5	34.9	-188.2
5mM	36.7	34.1	-193.7

On the basis of the effect of temperature on inhibition efficiency, the literature [49] distinguishes three types of inhibitors:

- Inhibitors showing a decrease in Inhibition efficiency with increase in temperature: E_a (uninhibited) < E_a (inhibited);
- Inhibitors showing no changes in inhibition efficiency with increase in temperature: E_a does not change with the presence and absence of the inhibitor;
- Inhibitors showing an increase in Inhibition efficiency with increase in temperature: E_a (uninhibited) > E_a (inhibited).

In our work, E_a(Blank) is greater than E_a (inhibited), what suggests the predominance of chemisorption. The positive signs of activation enthalpy changes (ΔH_a^*) obtained reflects the endothermic nature of the dissolution process. The shift toward negative values of activation entropy change (ΔS_a^*) in inhibited solutions [49] imply that the activated complex in the rate determining step represents an association rather than a dissociation, meaning that disordering decreases on going from reactants to the activated complex.

Quantum chemical calculations

The molecular structure with labels is given in **Figure 11**. The molecular structure of Theophylline in the ground state was optimized using B3LYP, B3PW91and PBEPBE hybrid functionals with 6-31G (d) basis set. The choice of

the best DFT method was based on the comparison of some experimental values of the structure parameters (bond angles, bond lengths), the CPU times and the total energy. Inhibition efficiency [50, 51] is correlated to the molecular and structural properties of inhibitor compounds. The molecular parameters in concern include HOMO (highest occupied molecular orbital) energy, LUMO (lowest unoccupied molecular orbital) energy, energy gap (ΔE) and the dipole moment μ. The calculated parameters with 6-31G (d) basis set are collected in **Tables 6A** and **B**.

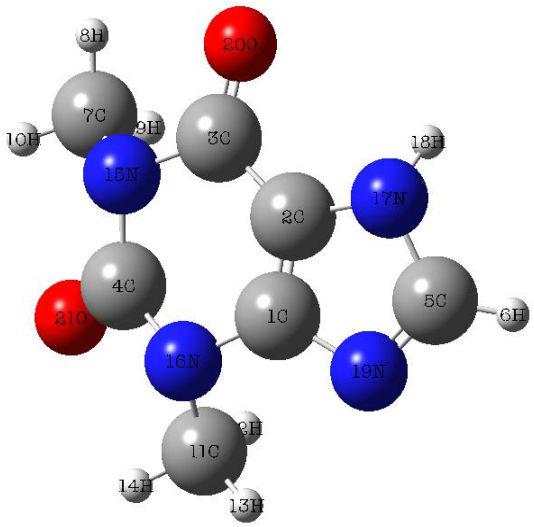

Figure 11 Optimized structure of Theophylline with labels by B3LYP/6-31G (d)

Table 6A Selected bond lengths and angles for different functionals

Length (Å, °)	B3LYP	B3PW91	PBEPBE	Experimental [52]
C(3)-N(15)	1.4173	1.4120	1.4277	1.4108
C(7)-N(15)	1.4662	1.4590	1.4648	1.4702
C(4)-O(21)	1.2223	1.2203	1.2319	1.2286
C(3)-O(20)	1.2265	1.2245	1.2369	1.2256
C(11)-N(16)	1.4623	1.4554	1.4619	1.4628
C(1)-N(19)	1.3639	1.3595	1.3695	1.3601
C(5)-H(6)	1.0813	1.0818	1.0895	0.9520
N(17)-H(18)	1.0105	1.0098	1.0183	0.9000
C(2)-C(3)-N(15)	110.7726	110.6597	110.3335	111.33
C(2)-N(17)-C(5)	106.5318	106.6052	106.7985	106.03
C(1)-N(16)-C(4)	119.6617	119.7024	119.9003	119.69
C(1)-N(19)-C(5)	103.9358	103.8351	103.6204	103.18

Table 6B Total energy and CPU times for different functionals

Descriptor	B3LYP	B3PW91	PBEPBE
Total energy(a u)	-641.062	-640.825	-640.342
CPU time	3h52’11”	8h18’19”	3h53’57”

The selected bond angles and bond lengths mentionned in tables 6 A have nearly the same values. It is not possible to choose the best method at this stage. Examining Table 6B, one can see that the lowest CPU time and the lowest ground state energy correspond to B3LYP functional which seems to be the appropriate functional for the calculations of the structural reactivity of theophylline. Indeed, the variational principle states that the ground state energy is the minimum energy:

$$E = min_n[F(n) + \int d^3 r V_{ext}(r) n(r)] \qquad (13)$$

Where $F(n)$, $V_{ext}(r)$ and $n(r)$ are respectively a universal functional, the external potential and the electronic density.

Reactivity and selectivity parameters

Density functional theory (DFT) [53] has been found to be successful in providing insights into the chemical reactivity and selectivity, in terms of global parameters such as electronegativity(χ), hardness(η), softness (S) and local ones as Fukui function $F(r)$ and local softness $s(r)$.

For an N-electrons system with total electronic energy (E) and external potential $v(r)$, chemical potential (μ_p) known as the negative of electronegativity (χ) [54] has been defined as the first derivative of (E) with respect to N at $v(r)$:

$$\mu_p = -\chi = \left(\frac{\partial E}{\partial N}\right)_{v(r)} \qquad (14)$$

Global reactivity parameters

According to DFT-Koopmans' theorem [55] the ionization potential I can be approximated as the negative of the HOMO energy:

$$I = -E_{HOMO} \qquad (15)$$

The negative of LUMO energy is related to the electron affinity A:

$$A = -E_{LUMO} \qquad (16)$$

Absolute electronegativity (χ) and the global hardness (η) of the inhibitor molecule [56] are approximated as follows:

$$\chi = \frac{I+A}{2} \qquad (17)$$

$$\eta = \frac{I-A}{2} \qquad (18)$$

As hardness, softness (S) another global chemical descriptor measuring the molecular reactivity and stability is given by:

$$S = \frac{1}{\eta} \qquad (19)$$

The chemical hardness fundamentally signifies the resistance towards the deformation or polarization of the electron cloud of the atoms, ions or molecules under a small perturbation of a chemical reaction. A hard molecule [57] has a large energy gap and a soft molecule has a small energy gap.

The global electrophilicity index (ω) [58] which is a measure of energy lowering due to maximal electron flow between donor and acceptor is expressed as follows:

$$\omega = \frac{\mu_p^2}{2\eta} \qquad (20)$$

This index measures the propensity of chemical species to accept electrons. A good nucleophile has lower values of μ_p and ω while a good electrophile is characterized by high values of the same parameters. This new reactivity index measures the stabilization in energy when the system acquires an additional electronic charge from the environment. Thus the fraction of electrons transferred from the inhibitor to the metallic surface, ΔN [59] is expressed as follows:

$$\Delta N = \frac{\chi Cu - \chi inh}{2(\eta Cu + \eta inh)} \quad (21)$$

Where χ_{Cu} and χ_{inh} denote the absolute electronegativity of copper and inhibitor molecule respectively. The theoretical values used are $\chi_{Cu} = 4.98\, eV/mol$ [60] and $\eta_{Cu} = 0$ [61].

Local reactivity indices

The condensed Fukui functions provide information about atoms in a molecule that have a tendency to either donate (nucleophilic character) or accept (electrophilic character) an electron or a pair of electrons. The nucleophilic and electrophilic Fukui function for an atom k [62] can be computed using a finite difference approximation as follows:

$$f_{k^+} = [q_k(N+1) - q_k(N)] \text{ for nucleophilic attack} \quad (22)$$

$$f_{k^-} = [q_k(N) - q_k(N-1)] \text{ for electrophilic attack} \quad (23)$$

Where $q_k(N+1)$, $q_k(N)$ and $q_k(N-1)$ are the charges of the atoms on the systems with $(N+1)$, (N) and $(N-1)$ electrons respectively. Using global softness, we can define the local softness as follows:

$$s(r) = f(r)S \quad (24)$$

All the calculated parameters are collected in **Table 7**.

Table7 Quantum Chemical descriptors for theophylline obtained with DFT at B3LYP/6-31G (d)

Quantum descriptor	Value with respect to B3LYP/6-31 G(d)
E_{HOMO}/eV	-6.071
E_{LUMO}/eV	-0.920
ΔE/eV	5.151
Dipole moment μ (D)	3.544
Ionization potential/eV	6.071
Electronic Affinity/eV	0.920
Electronegativity χ/eV	3.495
Global hardness η/eV	2.575
Global softness S/(eV)$^{-1}$	0.388
Fraction of electron transferred ΔN	0.288
Electrophyllicity index ω	2.371

The energy of the highest occupied molecular orbital (E_{HOMO}) [63] measures the tendency to donate electrons to appropriate acceptor species with lower energy empty molecular orbitals. Therefore, higher E_{HOMO} values facilitate adsorption and therefore inhibition by influencing the transport process through the adsorbed layer. In our work, the value of E_{HOMO} (-6.071 eV) which can be considered as a higher value when compared with the values of the literature [64, 65] could explain the good behavior of theophylline as a copper corrosion inhibitor in 1M HNO_3. E_{LUMO} is related to the ability of the molecule to accept electrons. **Figures 12A** and **B** show respectively the highest occupied molecular orbital (HOMO) and the lowest unoccupied molecular orbital (LUMO) of theophylline.

The analysis of Figure 12 shows that HOMO and LUMO densities are mainly distributed throughout the rings. The lower value of E_{LUMO} (-0.920 eV) indicates that Theophylline could accept electrons from d orbital of the metal. The energy gap (ΔE) between LUMO and HOMO [66, 67] is an important parameter as a function of reactivity of the inhibitor molecule towards the adsorption on the metallic surface. As (ΔE) decreases, the reactivity of the molecule increases, leading to increase in inhibition efficiency of the molecule. Lower values of the energy difference [68] will render good inhibition efficiency, because the energy to remove an electron from the last occupied orbital will be low. The dipole moment (μ) is another parameter of the electron distribution in a molecule and is the measure of the

polarity of a polar covalent bond. The lower value of the dipole moment [69] will favor an accumulation of the inhibitor in the surface layer and therefore inhibition efficiency. However, several authors [70, 71] state that the inhibition efficiency increases with increasing values of dipole moment. So in general [72], there is no significant relationship between the dipole moment values and inhibition efficiency. Ionization energy is a fundamental descriptor of the chemical reactivity of atoms and molecules. High ionization energy [72] indicates high stability and chemical inertness and small ionization leads to high reactivity of atoms and molecules. The low value of ionization energy (6.071 eV) of theophylline is surely the cause of its high inhibition efficiency.

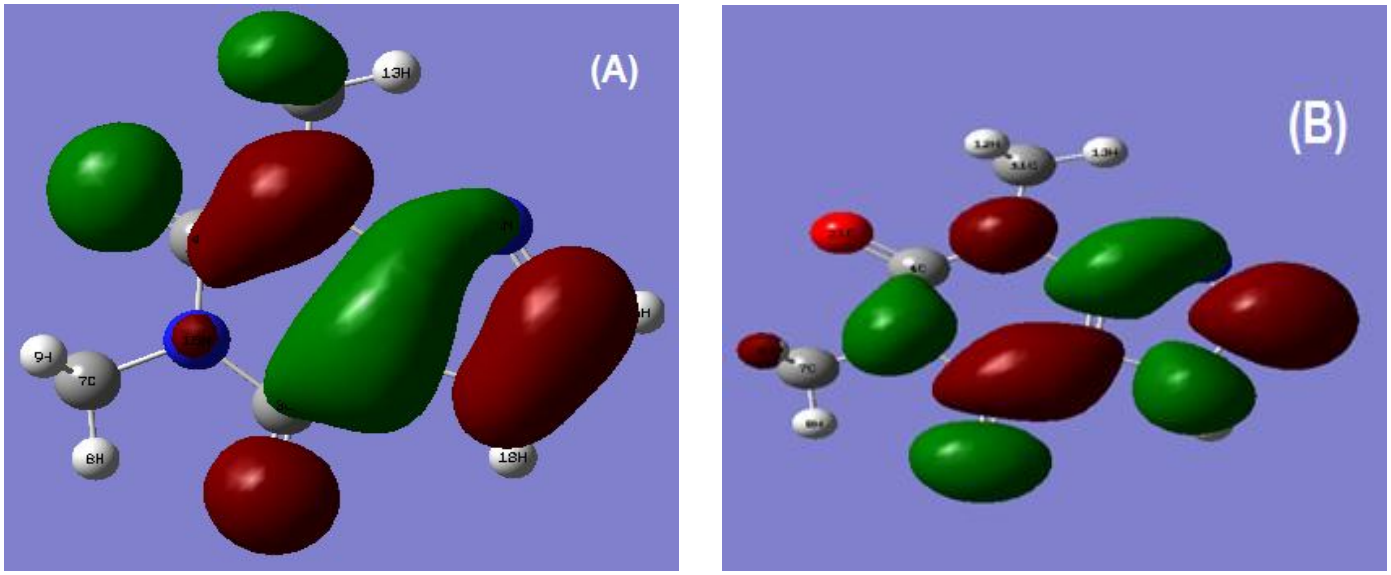

Figure 12 (A) HOMO of theophylline by B3LYP/6-31 G (d) **(B)** LUMO of theophylline by B3LYP/6-31 G (d)

Absolute hardness and softness are important properties to measure the molecular stability and reactivity. Theophylline has a low hardness value (2.575 eV) and a high softness value [0.388 $(eV)^{-1}$] what could explain its high inhibition efficiency.

Values of $\Delta N < 3.6$ [73] indicate that inhibition efficiency increases by increasing electron donating ability of the molecule to the metal surface. In our case, the value of ΔN is 0.288, what confirms the ability of (TP) to donate electrons to copper. The unoccupied d orbitals of Cu^{2+} ($[Ar]3d^9$) can accept an electron from the inhibitor to form coordinate bond.

The value of the electrophylicity index (2.371 eV) is low, what shows that the molecule has the capacity to accept electrons. The inhibitor molecule can accept electrons from Cu^{2+} ion with its antibonding orbitals to form back donating bond. These donation and back donation processes [74] strengthen the adsorption of the inhibitor molecule onto copper surface.

Several authors [75] state that the more negatively charged an heteroatom is, the more it can be adsorbed on the metal surface, through the donor-acceptor type reaction. One must consider the situation associated with a molecule that is going [76] to receive a certain amount of charge at some centre and is going to back donate a certain amount of charge through the same centre or another one.

Table 8 gives Fukui indices and the local softness indices. According to Parr and Yang [22] a larger value of Fukui function indicates more reactivity. Hence, greater the value of condensed Fukui function, the more reactive is the particular atomic centre in the molecule. The function f_k+ measures the changes of density when the molecule gains electrons and it corresponds to reactivity with respect to nucleophilic attack. On the other hand, f_k- corresponds to reactivity with respect to electrophilic attack or when molecule loss electron.

The preferred site for nucleophile attacks is around N (15) (Figure 12A), f_k+ is maximum what is confirmed by the lack of electron cloud around the nitrogen atom while the preferred site for electrophile attacks is near C (4) (Figure 12B) where f_k- has its maximum value.

Table 8 Fukui and local softness indices for nucleophilic and electrophilic attacks in theophylline

Atom N°	f_k^+	f_k^-	s_k^+	s_k^-
C1	-0.171643	0.041289	-0.06659748	0.01602013
C2	-0.075807	-0.018624	-0.02941312	-0.00722611
C3	-0.193786	0.033438	-0.07518897	0.01297394
C4	-0.096745	**0.063587**	-0.03753706	**0.02467176**
C5	-0.132362	-0.024549	-0.05135646	-0.00952501
H6	-0.087517	-0.093040	-0.03395660	-0.03609952
C7	0.028239	0.039174	0.01095673	0.01519951
H8	-0.038502	-0.040714	-0.01493878	-0.01579703
H9	-0.049899	-0.016458	-0.01936081	-0.00638570
H10	-0.036883	-0.057631	-0.01431060	-0.02236083
C11	0.033449	0.045178	0.01297821	0.01752906
H12	-0.044624	-0.042908	-0.01731411	-0.01664830
H13	-0.036007	-0.051486	-0.01397072	-0.01997657
H14	-0.038961	-0.070879	-0.01511687	-0.02750105
N15	**0.062196**	-0.109196	**0.02413205**	-0.04236805
N16	0.061122	-0.172740	0.02371534	-0.06702312
N17	0.014158	-0.098122	0.00549330	-0.03807134
H18	-0.060355	-0.043477	-0.02341774	-0.01686908
N19	-0.010133	-0.101495	-0.00393160	-0.03938006
O20	-0.102428	-0.135015	-0.03974206	-0.05238582
O21	-0.023512	-0.146331	-0.00912266	0.05677643

Conclusion

The results of this study can be concluded as follows:

- Theophylline is a good inhibitor for copper corrosion in 1 M HNO_3;
- The inhibition efficiency is temperature and concentration dependent;
- The molecule adsorbs on copper according to the modified Langmuir isotherm;
- The values of adsorption thermodynamic functions and that of the activated energy suggest both physisorption and chemisorption;
- The global reactivity descriptors confirm the good inhibition efficiency of theophylline;
- The Fukui indices lead to the nucleophilic attacks site (around N (15)) and electrophilic attacks site (near C (4)).
- Experimental and theoretical results are in good agreement.

References

[1] Furukawa Y, Kim J, Watkins J, Wilkin R T, Environ Sci Technol 2002, 36, 5469-5475.
[2] Umoren S A, Obot I B, Obi-Egbedi N O, Mater Sci 2009, 44, 274 -279.
[3] Badr GE, Corros Sci 2009, 51, 2529 -2536.
[4] Laarej K, Bouachrine M, Radi S, Kertit S, Hammouti B, E J Chem 2010, 7, 419- 424.
[5] Obot IB, Obi-Egbedi NO, Surface Review and Letters 2008, 15, 903-910.
[6] Abd El-Rehim S S, Ibrahim M A M, Khaled FFJ, Appl Electrochem1999, 29, 593-599.
[7] Antonijevic M M, Petrovic M B, Int Electrochem Sci 2008, 3, 1-28.
[8] Fallavena T, Antonov M, Gonçalves R S, Appl Surf Sci 2006, 253, 566-571.
[9] Rajendran S, Vaibhavi S, Anthony N, Trivedi D C, Corros Sci 2003, 59, 529-534.
[10] Eddy N O, Odoemelam S A, Adv Nat Appl Sci 2008, 2, 225-232.
[11] Eddy N O, Odoemelam S A, Ekwumemgbo P, Sci Res Essays 2009, 4, 33-38.
[12] Naqvi I, Saleemi A R, Naveed S, Int J Electrochem Sci 2011, 6, 146-161.

[13] Acharga S, Upadhyay S N, Trans Indian Inst Met 2004, 57,297-306.
[14] Eddy N O, Stoyanov S R, Ebenso E E, Int J Electrochem Sci 2010, 5, 1127-1150.
[15] Ebenso E E, Obot I B, Murulawa L C, Int J Electrochem 2010, 5, 1574-1586.
[16] Obot I B, Obi-Egbedi N O, Umoren S A, Corros Sci 2009, 51, 1868-1875.
[17] Bentiss F, Lebrini M, Lagrenee M, Corros Sci 2005, 47, 2915-2931.
[18] Vosta J, Eliasek J, Corros Sci 1971, 11, 223-229.
[19] Hohenberg P, Kohn W, Phys Rev B 1964, 136, 864-871.
[20] Parr R G, Yang W, Oxford University Press, New York, 1989, p105-110.
[21] Sanderson R T, J Am Chem Soc 1952, 74, 272-274.
[22] Parr R G, Yang W, J Am Chem Soc, 1984, 106, 4049-4050.
[23] Kohn W, Sham I J, Phys Rev A 1965, 140, 1133-1138.
[24] Geerlings P, De Proft F, Langenaeker W, Chem Rev 2003, 103, 1793-1873.
[25] Parr R G, Yang W, Ann Rev Chem 1995, 46, 701-708.
[26] Parr R G, Yang W, Oxford University Press and Clarendon Press, New York and Oxford 1989, p332.
[27] Fukui K, Yonezawa Y, Shingu H, J Chem Phys 1952, 20, 722-725.
[28] Ayers P W, Levy M, Theor Chem Acc 2000, 103, 353-360.
[29] Boulklah M, Hammouti B, Lagrenee M, Bentiss F, Corros Sci 2006, 48, 2831-2842.
[30] Mercer A D, Br Corros J 1985, 20, 61-70.
[31] Afidah A R, Kassim J, Recent Patents on Mater Sci 2008, 1, 223-231.
[32] De Souza F S, Spinelli A, Corros Sci 2009, 51, 642-649.
[33] Jr Frisch M J, Trucks G W, Schlegel H B, Scuseria G E, Robb M A, Cheeseman J R, Montgomery J A, Vreven T, Kudin K N, Burant J C, Millam J M, Iyengar S S, Tomasi J, Barone V, Mennucci B, Cossi M, Scalmani G, Rega N, Petersson G A, Nakatsuji H, Hada M, Ehara M, Toyota K, Fukuda R, Hasegawa J, Ishida M, Nakajima T, Honda Y, Kitao O, Nakai H, Klene M, Li X, Knox J E, Hratchian H P, Cross J, B, Adamo C, Jaramillo J, Gomperts R, Stratmann R E, Yazyev O, Austin A. J, Cammi R, Pomelli C, Ochterski J W, Ayala P Y, Morokuma K, Voth G A, Salvador P, Dannenberg J J, Zakrzewski V G, Dapprich S, Daniels A D, Strain M C, Farkas O, Malick D K, Rabuck A D, Raghavachari K, Foresman J B, Ortiz J V, Cui Q, Baboul A G, Clifford S, Cioslowski J, Stefanov B B, Liu G, Liashenko A, Piskorz P, Komaromi Martin I R L, Fox D J, Keith T Al-Laham M A, Peng C Y, Nanayakkara A, Challacombe M, Gill P M W, Johnson B, Chen W, Wong M W, Gonzalez C, Pople J A Gaussian 03, Revision B.05, Gaussian, Inc., Pittsburgh PA, 2003.
[34] Becke A D, J Chem Phys 1993, 98, 5648-5652.
[35] Lee C, Yang W, Parr R G, Phys Rev B 1988, 37, 785-789.
[36] Miehlich B, Savin A, Stoll H, Preuss H, Chem Phys Lett 1989, 157, 200-206.
[37] Perdew J P, Burke K, Wang Y, Phys Rev B 1996, 54, 16533-16539.
[38] Perdew J P, Burke K, Ernzerhof M, Phys Rev Lett 1997, 78, 1396-1396.
[39] Akalezi C O, Enenebaku C K, Oguzie E E, J Mater Environ Sci 2013, 4, 217-226.
[40] Moretti G, Quatarone G, Tassam A, Electrochimica Acta 1996, 41, 1971-1980.
[41] Essien E A, Umoren S A, Essien E E, Udoh A P, J Mater Environ Sci 2012, 3, 477-484.
[42] Villamil R F V, Corio P, Rubin J C, Agostinho S M L, J Electroanal Chem 1999, 472, 112-116.
[43] Keles H, Keles M, Dehri I, Serinday O, Colloids Surf A: Physicochem Eng Aspects 2008, 320, 138-145.
[44] Popova A, Sokolova E, Raicheva S, Christov M, Corrosion Science 2003, 45, 33-58.
[45] Durnie W, Marco R D, Jefferson A, Kinsella B, J Electrochem Soc 1999, 146, 1751-1756.
[46] Gemeay A H, El Sherbiny A S, Zaki A B, J Colloid Interface Sci 2002, 245, 116-125.
[47] Mall I D, Srivastava V C, Agarwal N K, Mishra I M, Colloids Surf A: Physicochem Eng Asp 2005,264, 17-28.
[48] Noor E A, Appl Electrochem 2009, 39, 1465-1475.
[49] Dehri I, Ozcan M, Mater Chem Phys 2010, 123, 666-677.
[50] Rodriguez-Valdez L, Martinez-Willafane A, Glossman-Mitnik, J Mol Struct (THEOCHEM) 2005, 716, 61-65.
[51] Lashkari M, Arshadi M R, Chem Phys 2004,299, 131-137.
[52] Cardin C, Gan Y, Lewis T, Acta Crist 2007, E63, o3175-o3175.
[53] Stoyonova A E, Peyerimhoff S D, Electrochim Acta 2002, 47, 1365-1371.
[54] Parr R G, Donelly R A, Levy M, Palke W E, J Chem Phys 1978, 68, 3801-3807.

[55] Koopmans T, Physica (Elsevier) 1934, 1, 104-113.
[56] Wang H, Wang X, Wang H, Wang L, Liu A, J Mol Model 2007, 13, 147-153.
[57] Fleming J, Frontier Orbitals and Organic Chemical Reactions, John Wiley and Sons, New York, 1976, p249.
[58] Parr R G, Szentpaly L, Liu S, J Am Chem Soc 1999, 121, 1922-1924.
[59] Pearson R G, Inorg Chem 1988, 27, 734-740.
[60] Pearson R G, Proc Natl Acad Sci USA 1986, 83, 8440-8441.
[61] Sastri V S, Perumareddi J R, Corrosion 1997, 53, 617-622.
[62] Eddy N O, Stoyanov S R, Ebenso E E, Int J Electrochem Sci 2010, 5, 1127-1150.
[63] Udhayakala P, Rajendiran T V, Gunasekaran S, Journal of Computational Methods in Molecular Design 2012, 2, 1-15.
[64] El Ouati I, Hammouti B, Aouniti A, Ramil Y, Azougagh M, Essasi E M, Bouachrine M, J Mater Envir Sci 2010, 1, 1-8.
[65] Hemapriya V, Parameswari K, Chitra S, Chemical Science Review Letters 2014, 3, 824-835.
[66] Herrag L, Hammouti B, Elkadiri S, Aouniti A, Jama C, Vezin H, Bentiss F, Corros Sci 2010, 52, 3042-3051.
[67] Obot I B, Obi Egbedi N O, Corros Sci 2010, 52, 198-204.
[68] Obot I B, Obi-Egbedi N O, Umoren S A, Int J Electrochem Sci 2009,4,863-877.
[69] Khalil N, Electrochimica Acta 2003, 48, 2635-2640.
[70] Khaled K F, Babic-Samardzija K, Hackerman N, Electrochimica Acta 2005, 50, 2515-2520.
[71] Bereket G, Hür E, Oretir C, Journal of Molecular Structure THEOCHEM 2002, 578, 1-3.
[72] Gece G, Corros Sci 2008, 50, 2981-2992.
[73] Lukovits I, Kalman E, Zucchi F, Corrosion, 2001, 3-8.
[74] Arslan T, Kandemirli F, Ebenso E E, Love I, Alemri H, Corros Sci 2009, 51, 35-47.
[75] Breket G, Hur E, Ogretir C, J Mol Struct (THEOCHEM) 2002, 578, 79-88.
[76] Gomez B, Likhanova N V, Dominguez-Aguilar M A, Martinez-Palou R, Vela A, Gasquez J, J Phys Chem 2006, 110, 8928-8934.

Publication History
Received 12th Feb 2016
Accepted 15th Mar 2016
Online 30th Oct 2016